

Thermally oxidized formation of new Ge dots over as-grown Ge dots in the Si capping layer

Tian-Xiao Nie, Jin-Hui Lin, Zhi-Gang Chen, Yuan-Min Shao, Yue-Qin Wu, Xin-Ju Yang, Yong-Liang Fan, Zui-Min Jiang^{*}, and Jin Zou^{*}

Citation: *Journal of Applied Physics* **110**, 114304 (2011); doi: 10.1063/1.3665398

View online: <http://dx.doi.org/10.1063/1.3665398>

View Table of Contents: <http://aip.scitation.org/toc/jap/110/11>

Published by the *American Institute of Physics*

AIP | Journal of
Applied Physics

Save your money for your research.
It's now **FREE** to publish with us -
no page, color or publication charges apply.

Publish your research in the
Journal of Applied Physics
to claim your place in applied
physics history.

Thermally oxidized formation of new Ge dots over as-grown Ge dots in the Si capping layer

Tian-Xiao Nie,^{1,2} Jin-Hui Lin,¹ Zhi-Gang Chen,² Yuan-Min Shao,¹ Yue-Qin Wu,¹ Xin-Ju Yang,¹ Yong-Liang Fan,¹ Zui-Min Jiang,^{1,a)} and Jin Zou^{2,3,a)}

¹State Key Laboratory of Surface Physics, Fudan University, Shanghai 200433, China

²Materials Engineering, The University of Queensland, Brisbane, Queensland QLD 4072, Australia

³Centre for Microscopy and Microanalysis, The University of Queensland, Brisbane, Queensland QLD 4072, Australia

(Received 22 August 2011; accepted 30 October 2011; published online 1 December 2011)

A Si-capped Ge quantum dot sample was self-assembly grown via Stranski-Krastanov mode in a molecular beam epitaxy system with the Si capping layer deposited at 300 °C. After annealing the sample in an oxygen atmosphere at 1000 °C, a structure, namely two layers of quantum dots, was formed with the newly formed Ge-rich quantum dots embedded in the oxidized matrix with the position accurately located upon the as-grown quantum dots. It has been found that the formation of such nanostructures strongly depends upon the growth temperature and oxygen atmosphere. A growth mechanism was proposed to explain the formation of the nanostructure based on the Ge diffusion from the as-grown quantum dots, Ge segregation from the growing oxide, and subsequent migration/agglomeration. © 2011 American Institute of Physics. [doi:10.1063/1.3665398]

I. INTRODUCTION

The arrival of nanometer technologies has led to the realization of quantum dot (QD) devices in the physical world.¹ Particularly, semiconductor QDs have shown great potential in the application of advanced optoelectronics, such as single-electron transistors,² nanocrystal nonvolatile memory,³ and advanced light-emitting devices,⁴ owing to their substantial quantum confinement effects and associated well-developed semiconductor technologies. Ge QDs, because of their high compatibility with the mature Si technology, have been widely investigated in the past decade.^{5,6} Devices based on Ge QDs, such as metal-oxide-semiconductor field-effect transistors⁷ and infrared detectors,⁸ have been developed. To pursue additional excellent performance and potential applications, the nanostructures based on Ge QDs need to be further exploited. One significant nanostructure, Ge QD embedded in a dielectric matrix (such as SiO₂) has demonstrated peculiar properties, which could potentially be used to fabricate optoelectronic,⁹ photovoltaic,¹⁰ and nonvolatile memory devices.¹¹

Different methods, such as oxidation of GeSi alloy films,¹² co-sputtering of Ge and SiO₂,¹³ electron beam evaporation,¹⁴ and ion implantation,¹⁵ have been utilized to grow the architecture of Ge QDs embedded in the SiO₂ matrix. The common structural characteristic is that the Ge QDs are randomly distributed in the SiO₂ matrix with non-uniform size.^{13,16} To realize practical applications, the Ge QDs need to be accurately controlled with the position, size, and density. However, the difficulty in the realization of these goals has prevented the exploration with further progress despite intensive studies of Ge QDs embedded in the SiO₂ matrix.

In this study, Ge QDs, embedded in SiO₂ matrix with the position accurately located upon the as-grown Ge QDs, were synthesized by directly annealing Si-capped Ge QDs grown by molecular beam epitaxy (MBE) in oxygen atmosphere. Through carefully designed comparative experiments and detailed structural characterizations using atomic force microscopy (AFM), transmission electron microscopy (TEM), and micro-Raman spectroscopy, a structural evolution model, based on the Ge surface diffusion from the as-grown QDs, Ge segregation from the growing oxide, and subsequent migration/agglomeration is proposed.

II. EXPERIMENT

The growth of Ge QDs was carried out in an ultrahigh vacuum MBE system (Riber Eva-32) with two electron-beam evaporators as Ge and Si sources. The base pressure of the chamber is 5×10^{-10} Torr. A *p*-type Si(001) wafer with a resistivity of 1–10 Ω cm was used as the substrate and its surface was chemically cleaned using the Shiraki method.¹⁷ After removing a protecting oxide layer on the substrate by annealing at 1000 °C for 10 min in the growth chamber, an 80-nm-thick Si buffer layer was grown on the substrate at 640 °C with a growth rate of 0.05 nm/s. For the Ge QD growth, a two-step growth method was employed to improve the uniformity of the Ge QDs, in which a 0.8-nm-thick Ge layer was deposited first, followed by a 5-min growth interruption before depositing another 0.05-nm-thick Ge layer. The growth temperature is 640 °C with a Ge growth rate of 0.01 nm/s. Because of inevitable Ge/Si intermixing at high growth temperature, the Ge QDs actually contains a certain amount of Si. Subsequently, a 30-nm-thick Si layer was capped on the Ge QDs at a relatively low temperature of 300 °C with a growth rate of 0.05 nm/s. After the deposition of the Si capping layer, the substrate was immediately cooled down to room temperature naturally. The oxygen annealing

^{a)}Authors to whom correspondence should be addressed. Electronic addresses: zmjiang@fudan.edu.cn and j.zou@uq.edu.au.

of the sample was carried out in a furnace equipped with a temperature controller and a quartz tube. After the furnace was heated to 1000 °C in the oxygen atmosphere, the sample was placed into the middle of the quartz tube and kept there for 5 min with a flow rate of 150 l/h, followed by cooling down to room temperature in the tube nozzle.

The morphologies of the Si-capped Ge QDs before and after annealing were investigated by AFM (Solver P47-MDT) in contact mode in air. The microstructural and nanochemical characteristics of the Ge QD sample were comprehensively characterized by TEM (Philips Tecnai F20) equipped with energy dispersive spectroscopy (EDS). Raman measurements (Jobin Yvon HR 800) were used to analyze the composition and strain in the Ge QD sample, which was performed with the 514.5-nm line of an argon-ion laser for excitation. An optical microscope was used to focus the laser beam on the sample with the beam diameter of 10 μm .

III. RESULTS AND DISCUSSION

Figure 1(a) is a typical AFM image of the as-grown Si-capped Ge QDs and shows that a large quantity of islands with a dome shape and good size uniformity were formed on the sample surface. The average base diameter and height of the islands are ~ 70 nm and 12 nm, respectively. To understand the microstructure of the sample, the cross-section TEM investigation was carried out and an example is shown in Fig. 1(b). As can be seen, Ge QDs (the dark parts) are buried in the Si capping layer, while on the surface, some islands accurately lie vertically with the Ge QDs. The morphology of the islands on the surface is similar to the buried Ge QDs, indicating that the surface mobility of the deposited Si is kinetically limited. The high-resolution TEM (HRTEM) image (refer to Fig. 1(c)) indicates that some planar defects appear in the islands of the Si capping layer surface. The formation of the defects is closely related to the buried Ge QDs.⁵ The sharp boundary of the Ge QD indicates that Ge/Si intermixing is kinetically limited at the growth temperature.

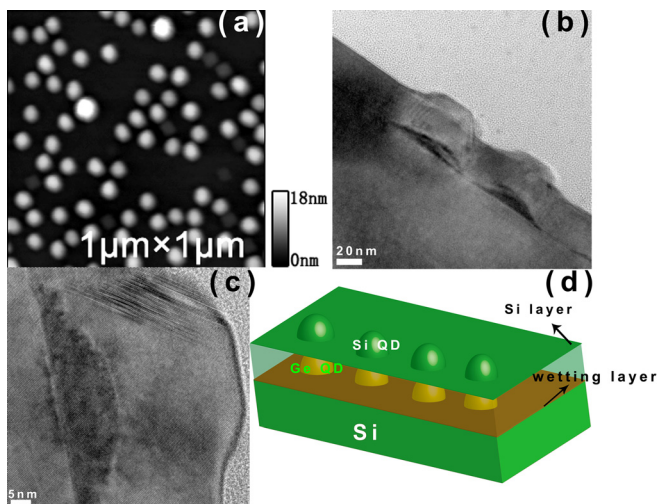


FIG. 1. (Color online) (a) AFM image of the as-grown Si-capped Ge QD sample; (b) and (c) the corresponding cross-sectional TEM and HRTEM images, respectively; (d) a stereo structural schematic illustration of the sample.

The base diameter and height of the Ge QD were ~ 54 nm and 12 nm, respectively. It should be mentioned that the difference in the island diameter observed by AFM and TEM is caused by the tip-broadening effect in the AFM measurement.¹⁸ Figure 1(d) is the schematic diagram of the observed sample structure.

After annealing at 1000 °C in oxygen atmosphere, the morphology of the sample was examined by AFM and an example is shown in Fig. 2(a). As can be seen, a large quantity of islands with a dome shape and good size uniformity exists on the surface of the annealed sample. The average base diameter and height of the islands are almost identical with that of the as-grown sample. The possible reason could be that the oxidation is homogeneous and independent on the surface morphology, so that the relative height of the islands remains after annealing. To evaluate the detailed microstructure of the annealed Si-capped Ge QD sample, TEM was carried out. Figure 2(b) is a typical bright-field TEM image of the annealed Si-capped Ge QD sample, which was collected in scanning transmission electron microscopy (STEM) mode. Based on the TEM contrast, two layers of QD structures were formed with newly formed QDs accurately located upon the as-grown QDs, whose base diameters increased slightly but height increased significantly up to 22 nm, in comparison with that of the as-grown sample. The blurred interface of the as-grown QDs indicates that the intermixing between the Ge and Si might take place during the annealing process. It should be mentioned that the as-grown Ge QDs may contain a certain amount of Si because of the diffusion of Si into the QDs during the high-temperature growth of Ge QDs.¹⁹ The post-annealing further promotes Si diffusion to the positions of as-grown Ge QDs. Except for the evolution of the QDs, a layer with lighter contrast is capped on the newly formed QDs and appears as an island morphology just upon the top layer of the newly

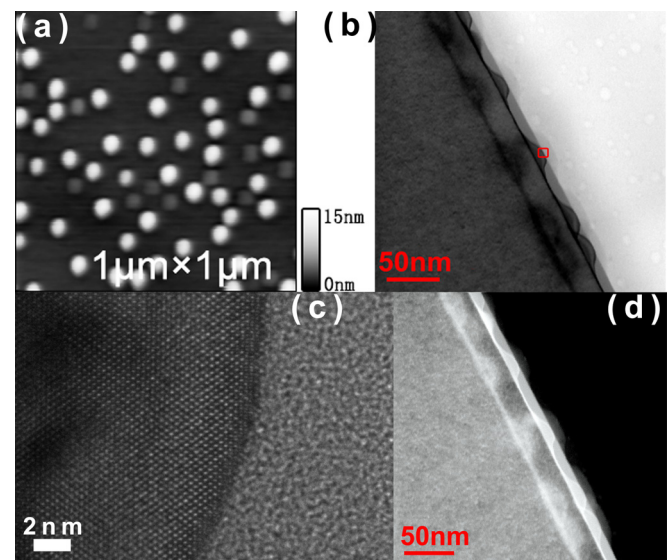


FIG. 2. (Color online) (a) AFM image of the sample annealed at 1000 °C. (b) The corresponding bright-field TEM image collected in STEM mode. (c) HRTEM image of one section of the annealing sample showing good crystallinity of the newly formed QDs. (d) HAADF of the annealed sample showing the Ge spatial distribution.

formed dots. To understand more detailed structural information, HRTEM was employed to characterize newly formed dots. Figure 2(c) is a HRTEM image of a section of a typical dot taken from the rectangle area (as shown in Fig. 2(b)) and shows that the newly formed QDs have good crystallinity with no lattice defects and the capping layer is amorphous. Our EDS analysis of the amorphous layer suggested that the amorphous capping layer is oxide, whose uniform thickness demonstrates that the oxidation is homogeneous, certifying our hypothesis of the oxidation homogeneity. To understand the compositional variations in the annealed sample, the high-angle annular dark field (HAADF) in the STEM mode was employed^{20,21} and a typical image is shown in Fig. 2(d). Based on the HAADF contrast, the newly formed QDs are much brighter than the as-grown QDs (which is just slightly brighter than the Si substrate), indicating that the newly formed QDs contain higher Ge concentrations (Ge atoms are much heavier than Si atoms). It should be noted that, after annealing, the HAADF contrast between the as-grown QDs and the Si substrate is small, suggesting that a significant amount of Ge in the as-grown QDs has been diffused away from the as-grown QDs toward the newly formed QDs.

To understand the observed phenomenon, other temperatures (namely 800 °C and 900 °C) were also chosen to anneal the as-grown Si-capped Ge QD samples. The Raman spectroscopy was also utilized to characterize the temperature-dependent Ge concentration in the samples, and typical examples are shown in Fig. 3(a). The spectra have been calibrated using a bulk Si first-order transverse optical peak of 520 cm^{-1} caused by the Si substrate,²² where all plots were shifted vertically for clarity. Two dashed lines were located at 302 cm^{-1} and 436 cm^{-1} , respectively. The broad peak centered around 302 cm^{-1} can be attributed to the overlap of Si two-order transverse acoustic peak and Ge-Ge peak.²³ It is of interest to

note that a Raman peak centered at 292 cm^{-1} can clearly be seen for the sample annealed at 1000 °C only. This peak corresponds to the Ge-Ge peak,²⁴ suggesting that the Ge-rich dots can be formed when annealing the sample reaches 1000 °C. The other peak (caused by Ge-Si phonon vibration mode²⁵), varied between 409 cm^{-1} and 423 cm^{-1} for different cases, can be observed, and variations of the peak position and the peak intensity are attributed to the variation of chemical compositions and strains involved in different cases. The fact that the intensity of the Ge-Si peak in the sample annealed at 900 °C is lower than that in the sample annealed at 800 °C indicates that the Ge concentration in the QDs is decreased and a more intense Ge/Si intermixing took place during the annealing at 900 °C.²⁵ Interestingly, the sample annealed at 1000 °C shows a different behavior, in which a very strong intensity of the Ge-Si peak was increased in comparison with samples annealed in other temperatures (note that the intensity of the Ge-Ge peak centered at 292 cm^{-1} is also very strong), indicating that the Ge-rich QDs were formed at 1000 °C,²⁴ agreeing with our TEM results. In our annealing process, the oxygen plays an important role for the formation of Ge-rich QDs. To verify this conclusion, the forming gas (95% N_2 and 5% H_2) was used to anneal the as-grown Si-capped Ge QD samples, under identical annealing conditions. The Raman spectroscopy was used to examine the newly annealed sample, and an example is shown in Fig. 3(b). As can be seen, both the Ge-Ge peak and the Ge-Si peak are very weak, indicating that solely intense Ge/Si intermixing occurs with no newly formed Ge-rich QDs under the annealing in the forming gas at 1000 °C. The microstructure of the sample annealed in the forming gas was further characterized by bright-field TEM in STEM mode, and a typical example is shown in Fig. 3(c). Based on the TEM contrast, no oxide layer and newly formed Ge QDs can be observed, which exhibits a distinct

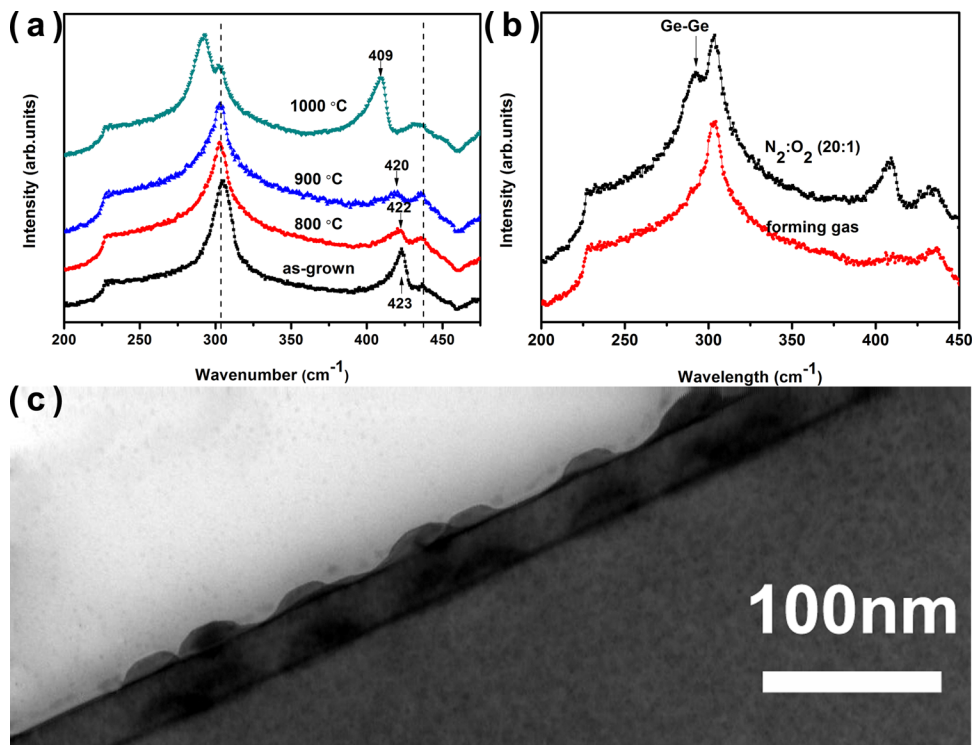


FIG. 3. (Color online) (a) Raman spectra of the as-grown Si-capped Ge QD samples annealed at different temperatures. (b) Raman spectra of the as-grown Si-capped Ge QD samples annealed at 1000 °C in forming gas and mixed gas of 95% N_2 and 5% O_2 , respectively, showing a totally different behavior compared with that in pure oxygen. (c) The STEM mode-collected bright-field TEM image of the as-grown Si-capped Ge QD sample annealed at 1000 °C in forming gas.

microstructure feature with that in the oxygen-annealed sample. The blurred interface of the as-grown Ge QDs indicates that intense Ge/Si intermixing took place during the annealing process in forming gas, which is consistent with our Raman results. Furthermore, in comparison with the as-grown sample, we found that the base diameter of the Ge QDs increased slightly but its height increased significantly, which is similar to the changing behavior in the oxygen-annealed sample.

Taking all the above experimental results into account, we can conclude that the fact that Ge in the as-grown QDs has diffused into the newly formed QDs can only be realized when the as-grown Si-capped Ge QDs are annealed under the oxygen atmospheres at 1000 °C. To understand the formation mechanism of such an extraordinary physical phenomenon, two points should be clarified: (1) selective oxidation of Si in the Ge/Si alloys, and (2) Ge diffusion toward the surface during the annealing process. The preferential oxidation of Si is because of the higher binding energy of Si and O compared to that of Ge and O.²⁶ To understand the Ge diffusion toward the surface, we note that: (1) The tensile strain in the Si capping layer over the Ge QDs should enhance the Ge/Si interdiffusion, resulting in the Ge diffusion mainly vertically toward the Si capping layer,²⁵ which has been observed both in oxygen- and forming gas-annealed samples. (2) The planar defects in the Si capping layer (including surface islands) in the as-grown sample may attract Ge atoms.^{27,28} We anticipate that a formation mechanism of newly formed QDs is caused by the synergetic effect of the Ge/Si interdiffusion, Ge segregation from the oxide, and subsequent migration/agglomeration.¹² It is well documented that the diffusion coefficient is exponentially proportional to the environmental temperature, and the diffusion length of Ge can then be estimated. Using Ge diffusion coefficient of $\sim 2 \times 10^{-14}$ cm²/s in Si,^{29,30} the diffusion length of Ge is estimated as ~ 25 nm at 1000 °C for 5 min (our annealing condition). Meanwhile, the oxidation rate is proportional to the environmental temperature. Based on these considerations, when annealing at lower growth temperature, the Ge diffusion to the sample surface should be restricted, consequently inducing a smaller amount of Ge on the sample surface, so that the Ge–Ge peak in the Raman spectra cannot be seen at the lower growth temperature of 800 °C and 900 °C. In contrast, when annealing at a higher temperature (i.e., 1000 °C), the Ge diffusion to the surface should be substantially enhanced. Meanwhile, the increased oxidation rate at higher temperature leads to a thicker oxide layer; and the simultaneous expelling of Ge in the oxide layer promotes the formation of QDs via subsequent Ge migration/agglomeration.

To further certify this mechanism, the as-grown Si-capped Ge QD sample was annealed in diluted oxygen gas (95% N₂ and 5% O₂) at 1000 °C for 10 min. As expected, a weak Ge–Ge peak in the Raman spectrum can be seen (refer to Fig. 3(b)), which is overlapped on the Si two-order acoustic phonon peak. This experimental result confirms our conclusion.

Based on the discussion outlined above, Fig. 4 illustrates the evolutionary model schematically. At a low growth temperature, the weak Ge/Si intermixing would induce a small amount of Ge diffusion to the sample surface. Meanwhile, the restricted oxidation rate would lead to a thin oxide layer

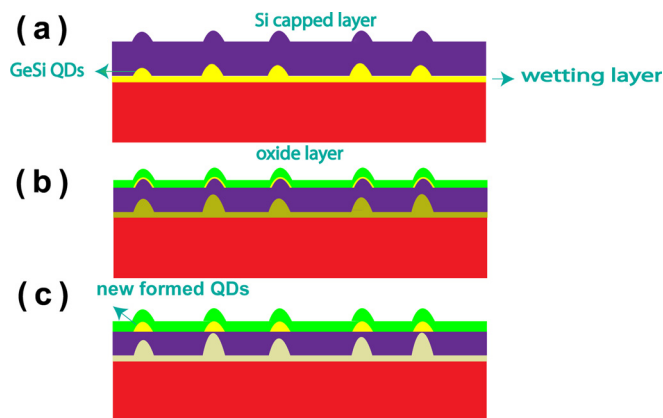


FIG. 4. (Color online) Schematic illustrations of the evolution of as-grown Si-capped Ge QD sample with the temperature variation. (a) As-grown sample. (b) Annealed at low temperature. (c) Annealed at high temperature.

on the sample surface, thereby driving a small quantity of Ge to segregate from the oxide, as illustrated in Fig. 4(b). In comparison, at a high growth temperature, the intense Ge/Si intermixing would induce a large amount of Ge diffusion to the sample surface. The intensely increased oxide thickness would segregate much more Ge to agglomerate beneath the oxide layer in the form of QDs. The corresponding schematic illustration is shown in Fig. 4(c).

IV. CONCLUSION

A nanostructure, namely, newly formed Ge-rich QDs embedded in the SiO₂ matrix with the positions accurately located upon the as-grown QDs, was formed by directly annealing Si-capped Ge QDs in an oxygen atmosphere at 1000 °C. The formation of this nanostructure is closely related to the growth temperature and oxygen atmosphere. Through carefully designed comparative experiments, a growth mechanism based on the Ge diffusion from the as-grown QDs, Ge segregation from the growing oxide, and subsequent migration/agglomeration is proposed to explain the formation of the nanostructure.

ACKNOWLEDGMENTS

This work is supported by the special funds for the Major State Basic Research Project (No. 2011CB925601) of China, the NSFC under Grant No. 10874026, and the Australian Research Council.

¹Y. W. Chen, B. Y. Pan, T. X. Nie, P. X. Chen, F. Lu, Z. M. Jiang, and Z. Y. Zhong, *Nanotechnology* **21**, 175701 (2010).

²P. Li, D. Kuo, W. Liao, and W. Lai, *Appl. Phys. Lett.* **88**, 213117 (2006).

³J. H. Wu and P. W. Li, *Semicond. Sci. Technol.* **22**, S89 (2007).

⁴V. Craciun, C. Boulmer-Leborgne, E. J. Nicholls, and I. W. Boyd, *Appl. Phys. Lett.* **69**, 1506 (1996).

⁵J. H. Lin, Y. Q. Wu, J. Cui, Y. L. Fan, X. J. Yang, Z. M. Jiang, Y. Chen, and J. Zou, *J. Appl. Phys.* **105**, 024307 (2009).

⁶Y. Q. Wu, J. Zou, F. H. Li, J. Cui, J. H. Lin, R. Wu, and Z. M. Jiang, *Nanotechnology* **18**, 025404 (2007).

⁷A. Yakimov, A. Dvurechenskii, V. Kirienko, and A. Nikiforov, *Appl. Phys. Lett.* **80**, 4783 (2002).

⁸A. I. Yakimov, A. V. Dvurechenskii, A. I. Nikiforov, and Y. Y. Proskuryakov, *J. Appl. Phys.* **89**, 5676 (2001).

⁹R. J. Walters, G. I. Bourianoff, and H. A. Atwater, *Nature Mater.* **4**, 143 (2005).

- ¹⁰G. Conibeer, M. Green, R. Corkish, Y. Cho, E.-C. Cho, C.-W. Jiang, T. Fangsuwannarak, E. Pink, Y. Huang, T. Puzzer, T. Trupke, B. Richards, A. Shalav, and K.-L. Lin, *Thin Solid Films* **511-512**, 654 (2006).
- ¹¹W. K. Choi, W. K. Chim, C. L. Heng, L. W. Teo, V. Ho, V. Ng, D. A. Antoniadis, and E. A. Fitzgerald, *Appl. Phys. Lett.* **80**, 2014 (2002).
- ¹²W. Lai and P. Li, *Nanotechnology* **18**, 145402 (2007).
- ¹³W. K. Choi, H. G. Chew, F. Zheng, W. K. Chim, Y. L. Foo, and E. A. Fitzgerald, *Appl. Phys. Lett.* **89**, 113126 (2006).
- ¹⁴P. Basa, G. Molnár, L. Dobos, B. Pécz, L. Tóth, A. Tóth, A. Koós, L. Dózsa, A. Nemcsics, and Z. Horvath, *J. Nanosci. Nanotechnol.* **8**, 818 (2008).
- ¹⁵S. Mestanza, E. Rodriguez, and N. Frateschi, *Nanotechnology* **17**, 4548 (2006).
- ¹⁶N. L. Rowell, D. J. Lockwood, A. Karmous, P. D. Szkutnik, I. Berbezier, and A. Ronda, *Superlattices Microstruct.* **44**, 305 (2008).
- ¹⁷A. Ishizaka and Y. Shiraki, *J. Electrochem. Soc.* **133**, 666 (1986).
- ¹⁸D. L. Sedin and K. L. Rowlen, *Appl. Surf. Sci.* **182**, 40 (2001).
- ¹⁹X. Z. Liao, J. Zou, D. J. H. Cockayne, J. Wan, Z. M. Jiang, G. Jin, and K. L. Wang, *Phys. Rev. B* **65**, 153306 (2002).
- ²⁰J. Wall, J. Langmore, M. Isaacson, and A. Crewe, *Proc. Natl. Acad. Sci. U.S.A.* **71**, 1 (1974).
- ²¹N. Browning, D. Wallis, P. Nellist, and S. Pennycook, *Micron* **28**, 333 (1997).
- ²²T.-X. Nie, Z.-G. Chen, Y.-Q. Wu, J.-L. Wang, J.-Z. Zhang, Y.-L. Fan, X.-J. Yang, Z.-M. Jiang, and J. Zou, *J. Phys. Chem. C* **114**, 15370 (2010).
- ²³J. H. Lin, H. B. Yang, J. Qin, B. Zhang, Y. L. Fan, X. J. Yang, and Z. M. Jiang, *J. Appl. Phys.* **101**, 083528 (2007).
- ²⁴A. Kolobov, K. Morita, K. Itoh, and E. Haller, *Appl. Phys. Lett.* **81**, 3855 (2002).
- ²⁵J. Wan, Y. Luo, Z. Jiang, G. Jin, J. Liu, K. Wang, X. Liao, and J. Zou, *J. Appl. Phys.* **90**, 4290 (2001).
- ²⁶D. K. Nayak, K. Kamjoo, J. S. Park, J. C. S. Woo, and K. L. Wang, *Appl. Phys. Lett.* **57**, 369 (1990).
- ²⁷A. Kinomura, J. S. Williams, J. Wong-Leung, M. Petracic, Y. Nakano, and Y. Hayashi, *Appl. Phys. Lett.* **73**, 2639 (1998).
- ²⁸B. Mohadjeri, J. Williams, and J. Wong Leung, *Appl. Phys. Lett.* **66**, 1889 (1995).
- ²⁹B. Hollander, R. Butz, and S. Mantl, *Phys. Rev. B* **46**, 6975 (1992).
- ³⁰G. L. McVay and A. R. DuCharme, *J. Appl. Phys.* **44**, 1409 (1973).